npj | climate and atmospheric science

www.nature.com/npjclimatsci

ARTICLE OPEN

Check for updates

Arabian Sea Aerosol-Indian Summer Monsoon Rainfall relationship and its modulation by El-Nino Southern Oscillation

Gopinath Nandini[1], V. Vinoj[1]✉ and Satyendra Kumar Pandey[1]

The intensity of Indian summer monsoon rainfall (ISMR) over Central India (CI) is known to be positively correlated with the dust aerosol loading over the Arabian Sea (AS) on short time scales of about a week. However, global oscillations such as the El-Nino Southern Oscillation (ENSO) modulate both the rainfall over India and aerosol loading over the AS. This study uses long-term satellite-based aerosol and gridded rainfall datasets to explore the correlation between AS aerosol and CI rainfall and their relationship to ENSO. It is found that the highest correlation is during El-Nino (0.53), followed by Normal (0.44) and La-Nina (0.34) years, closely following the overall dust aerosol loading over the AS. Spatially, irrespective of the phase of ENSO, the high aerosol loading conditions are associated with increased winds over the AS, shifting eastward towards the Indian mainland and enhancing rainfall over CI and elsewhere across the Indian landmass. In contrast, the low aerosol loading conditions over the AS are associated with reduced winds, shifting westward away from the Indian mainland, suppressing rainfall over CI. In response to anthropogenic climate change, the El-Nino-like conditions are likely to increase in the future, making the dust aerosol-induced monsoon rainfall enhancement/modulation significant.

npj Climate and Atmospheric Science (2022)5:25 ; https://doi.org/10.1038/s41612-022-00244-8

INTRODUCTION

The atmospheric aerosols can modulate Earth's climate directly by scattering and absorbing the incoming solar and outgoing terrestrial longwave radiation[1–3] and indirectly by acting as cloud condensation nuclei and ice nuclei, thereby modifying the overall cloud properties[4–6]. Aerosols impact the local, regional and global climate at different temporal and spatial scales through these effects. They also modulate the Indian summer monsoon rainfall (ISMR) through multiple pathways[7–13]. For example, solar dimming induced by anthropogenic aerosols over the northern hemisphere slows down monsoon circulation by altering the north-south surface temperature gradient, reducing rainfall over the Indian region[14]. This mechanism has been responsible for changes in monsoon rainfall since the second half of the 20th century. On the other hand, the atmospheric absorption by aerosols such as dust and black carbon during the pre-monsoon season enhances early monsoon rainfall by the elevated heat pump hypothesis (EHP)[15,16]. The physical mechanism underlying the delayed response in monsoon rainfall to pre-monsoon aerosol loading through EHP still eludes the scientific community[17–20]. Against this backdrop, a study showed that remote aerosols over West Asia/North Africa and the Arabian Sea(AS) modulate monsoon rainfall on short time scales of about a week[21]. The hypothesis states that the dust aerosols accumulated over the AS cause atmospheric warming to strengthen the monsoon circulation, leading to increased monsoon rainfall over Central India (CI) in about a week. Following this, few other studies using extensive satellite-based measurements and simulations conducted by global and regional climate models supported these findings and suggested similar hypotheses and a few different variants[22–24]. In addition, in the future warming scenarios, studies have indicated that the positive correlation between dust loading over the AS and rainfall over India may likely strengthen due to the increased wind speed over the dust-source regions leading to increased transport of aerosols[25]. Thus, the Indian monsoon rainfall is modulated by remote dust feedback to a certain extent.

The ENSO significantly impacts both the ISMR and dust loading over the AS. The El-Nino years are associated with deficit rainfall, and most of the La-Nina years are associated with surplus rainfall over India during the monsoon period[26,27]. Studies have also shown that the changes in the circulation patterns and rain associated with ENSO affect the emission and transport of dust aerosols from nearby dust-source regions to AS[28,29]. Therefore, changes in ENSO phases may alter the strength of the AS dust-monsoon relationship with implications to monsoon rainfall.

Some studies have explored the effect of ENSO in modulating the EHP mechanism over the Tibetan Plateau[30,31]. However, no observational studies have examined the relationship between Arabian Sea aerosols and Indian monsoon rainfall and its sensitivity to ENSO. Also, recent studies have indicated that El-Nino-like conditions will increase in the future due to anthropogenic climate change[32,33]. Therefore, it is essential to understand how ENSO may modulate the relationship between AS dust aerosol and monsoon rainfall. Thus the primary objective of this study is to explore how different phases of ENSO modulate the strength of the correlation between AS aerosols and CI precipitation.

RESULTS AND DISCUSSION

The correlation between the AS aerosols and CI rainfall

A study first reported the short-term correlation between aerosol loading over the AS and monsoon rainfall over CI[21]. They used 10 years of daily/weekly mean aerosol and rainfall datasets to reveal this relationship. In this paper, the first step is to identify whether this correlation could be captured by legacy aerosol datasets such

[1]School of Earth, Ocean and Climate Sciences, Indian Institute of Technology Bhubaneswar, Bhubaneswar, Odisha 752 050, India. ✉email: vinoj@iitbbs.ac.in

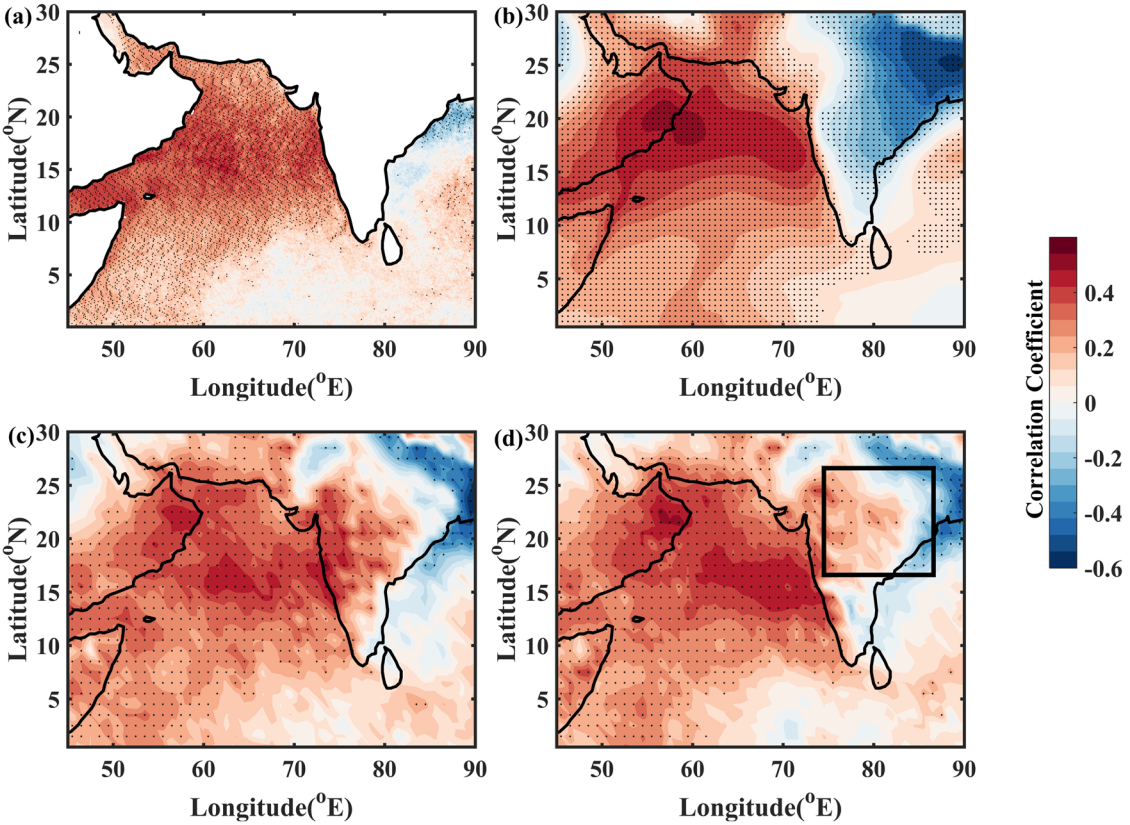

Fig. 1 Observed spatial correlation between AS aerosols and CI rainfall. The spatial pattern of the correlation coefficient between weekly mean AOD over AS and rain over CI (region inside the box) for **a** AVHRR(1981–2013), **b** MERRA-2(1981–2013), **c** MODIS-Aqua (2002–2013) and **d** MODIS-Terra (2000–2013). The black dots represent the statistical significance at 95% confidence level.

as the National Oceanic and Atmospheric Administration – Advanced Very High-Resolution Radiometer (NOAA-AVHRR), reanalysis such as Modern-Era Retrospective analysis for Research and Application (MERRA), and gridded observational rainfall data from the India Meteorological Department (IMD).

Figure 1 shows the spatial correlation patterns (between weekly mean aerosol loading over the AS and rainfall over CI) using four different Aerosol Optical Depth (AOD) datasets (AVHRR, MERRA, Moderate Resolution Imaging Spectroradiometer (MODIS) -Terra and Aqua) during the monsoon season from June to September (JJAS). The spatial pattern of correlation of AOD at each grid point over the AS with ISMR spatially averaged over CI is captured by AVHRR AODs (Fig. 1a). The maximum positive correlation is over the north-central AS (10–25°N and 50–75°E). The correlation patterns are similar to those reported using satellite measurements and climate model simulations[21]. Using the general circulation model CAM5 (Community Atmosphere Model), Vinoj et al. [21] showed that only dust aerosols could produce such positive correlation patterns. The correlation values also decrease towards the South of AS. While Fig. 1 shows a positive correlation between AOD over the AS, Arabian Peninsula, and West Asia, a low or negative correlation is seen over the Eastern Indian region. The similarity in correlation patterns between AVHRR and other aerosol datasets such as MODIS and MERRA reconfirms previous findings, thereby providing confidence in using AVHRR-AOD in the analysis and inferences made in the later sections.

The AOD over the Arabian Sea is dominated by sea salt and dust during the monsoon season[17,34,35]. Studies based on ship-based measurements have shown that sea-salt aerosols contribute to 20–60% of the total aerosol loading over the AS[36]. More recent studies[17] suggest that the AS has the highest aerosol loading during the monsoon season, with up to 80% of measurements identified as either desert dust or contaminated/polluted dust. Following this, another study[22] found that desert dust aerosols contribute to 53% of the total AOD over the AS. Detailed back trajectory analysis has shown that aerosols over North AS are transported from nearby dust-source regions, e.g. the Arabian Peninsula, the Horn of Africa, Iran, Iraq and Indo-Pak deserts. Only aerosols from the Horn of Africa are transported to the Southern AS, resulting in lower dust concentration and lower total column AOD[34]. These studies indicate that natural dust aerosols dominate the AS during the monsoon season in addition to the locally emitted sea-salt aerosols. Thus changes in dust transport from the adjoining regions are expected to modulate the aerosol loading and the correlation patterns over the AS. Therefore, their sensitivity to different phases of ENSO is explored in the succeeding sections. Any reference to correlation hereon would mean the correlation between aerosol loading over the AS and rainfall over the CI region unless specified.

The impact of ENSO on the observed correlation over the AS

There are numerous local, regional, and global factors that affect the interannual variability and strength of the monsoon. Especially, the influence of ENSO on ISMR has been a subject of considerable interest[37–41]. The El-Nino years are associated with deficit rainfall (including drought conditions), whereas La-Nina years are related to excess rainfall (including floods) over the Indian region. Similarly, dust transport over the AS depends upon the strength and direction of winds over the adjacent desert regions[29]. Past studies have reported that winter La-Nina leads to a negative precipitation anomaly over the West Asian/Arabian Peninsular regions and results in more dust generation and emissions in the following summer[28,42]. Another study using monthly mean Aerosol Index (AI) and Oceanic Nino Index (ONI)

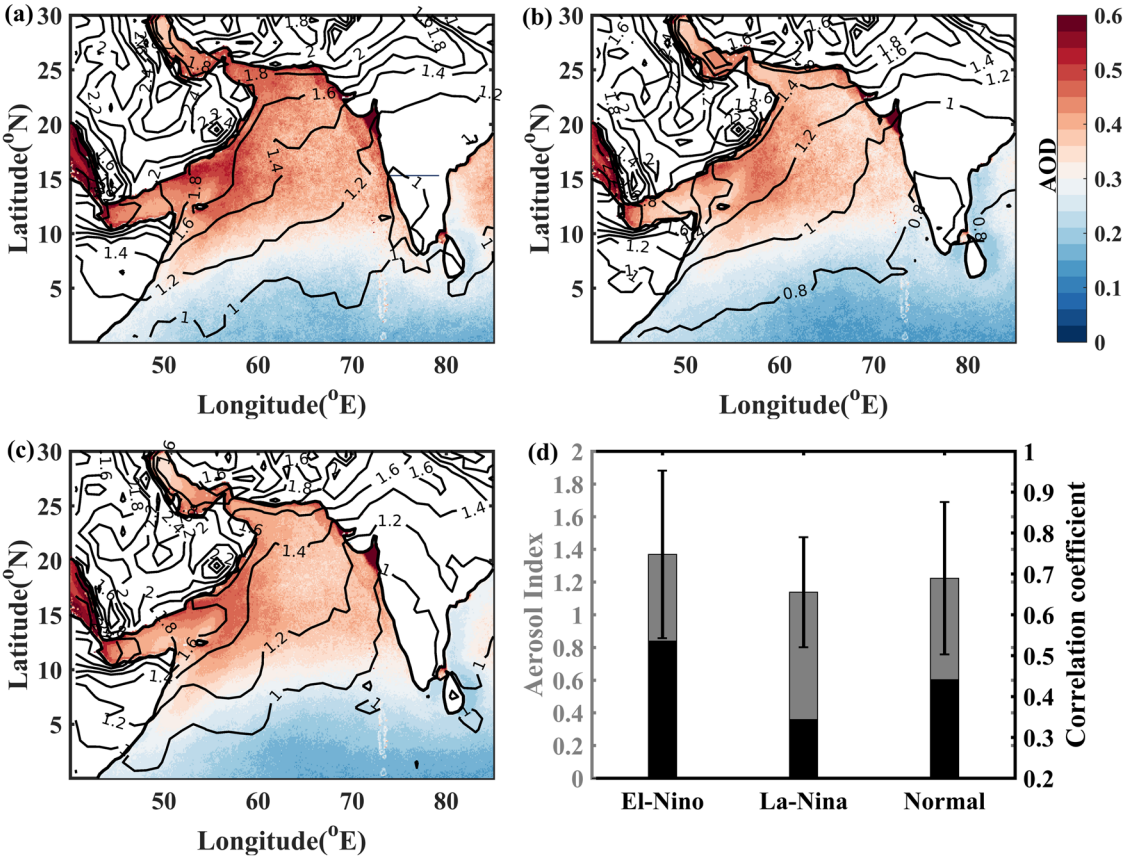

Fig. 2 Spatial pattern of AOD and Aerosol Index over the AS. a El-Nino, **b** La-Nina and **c** Normal years. The colour bar shows the AOD, and the contour lines indicate AI. **d** The black bar represents the correlation coefficient calculated for weekly mean AOD over the AS(10–25°N and 50–75°E) and the CI region separately for El-Nino (7 years, sample size $n = 121$), La-Nina (8 years, $n = 139$) and Normal years ($n = 309$) during the period 1981–2013. The grey bars represent the Spatio-temporal mean of AI over the AS and one standard deviation. Values of correlation coefficients are statistically significant above 95% confidence level.

from October to May showed that during El-Nino conditions, warm SST anomalies over the Pacific Ocean remotely cause the zonal circulation to be pronounced with well-defined areas of rising motion over the Arabian Peninsula and sinking motion over the Indian subcontinent resulting in an overall reduction in monsoon rainfall. At the same time, the intense westerly at 700hPa during El-Nino transports large quantities of dust aerosols from the Arabian Peninsula towards the East to the AS. In contrast, a weak and less organized zonal circulation system associated with cold SST anomalies over the Pacific Ocean suppresses the aerosol loading during the La-Nina phase over the AS[29]. Thus, it is clear that ENSO simultaneously alters the intensity of ISMR and dust aerosol loading over the AS.

One more aspect that needs to be clarified is the use of different ENSO indices based on the application in various studies. For example, a study conducted to explore the impact of ENSO on the aerosol loading over the Indo-Gangetic Plain (IGP) and Tibetan Plateau and on the EHP mechanism showed increased (decreased) aerosol loading over Northern India during La-Nina (El-Nino), leading to the amplification of the ISMR[30]. Whereas another study showed that, during pre-monsoon, enhanced loading of absorbing aerosols over the IGP could reduce the severity of drought during El-Nino years by invoking the EHP mechanism[31]. Thus, one study states that increased aerosol (over North India and Tibetan Plateau) during La-Nina increases rainfall due to strengthened EHP (pre-monsoon ENSO indices). Still, another study shows an enhancement in aerosol loading during El-Nino leading to increased rainfall, thereby suppressing the effect of drought that often prevails during the El-Nino period over India (monsoon ENSO indices). Although both studies show rain enhancement due to higher aerosol loading, their conclusion shows aerosol-induced rainfall enhancement at different ENSO phases. This disagreement is attributable to the difference in the years considered as El-Nino/La-Nina in these studies due to the different periods used to extract the ENSO indices.

Though El-Nino peaks during the winter season, previous studies have shown that the simultaneous effect of ENSO on ISMR is stronger than the delayed impact[40,43,44]. Therefore, it is essential to use simultaneous ENSO indices to avoid ambiguity in interpreting the results from various studies. This study considers the ENSO indices concurrent to the monsoon season (see data and methods section for more details).

Figure 2a–c shows aerosol loading over the AS during different phases of ENSO, El-Nino, La-Nina, and Normal. The years classified into El-Nino and La-Nina are 1982, 1987, 1991, 1997, 2002, 2004, 2009 and 1985, 1988, 1998, 1999, 2000, 2007, 2010, 2011, respectively, based on the ONI (see also data and methods section) during JJAS. The spatial gradients (north-west to south-east for both AOD and AI) indicate that the dust primarily contributes to the variability in the aerosol loading. It can be seen that the AI values, which are more sensitive to absorbing aerosols like dust, are higher over the Arabian Peninsula and the AS during El-Nino compared to La-Nina and Normal years. The correlation between aerosol loading over the AS and rainfall over CI are calculated separately for each of the three ENSO phases (see Fig. 2d). The correlation is highest during El-Nino (0.53), followed by Normal (0.44) and La-Nina (0.34) years. The fact that all three phases show statistically significant correlation indicates that the

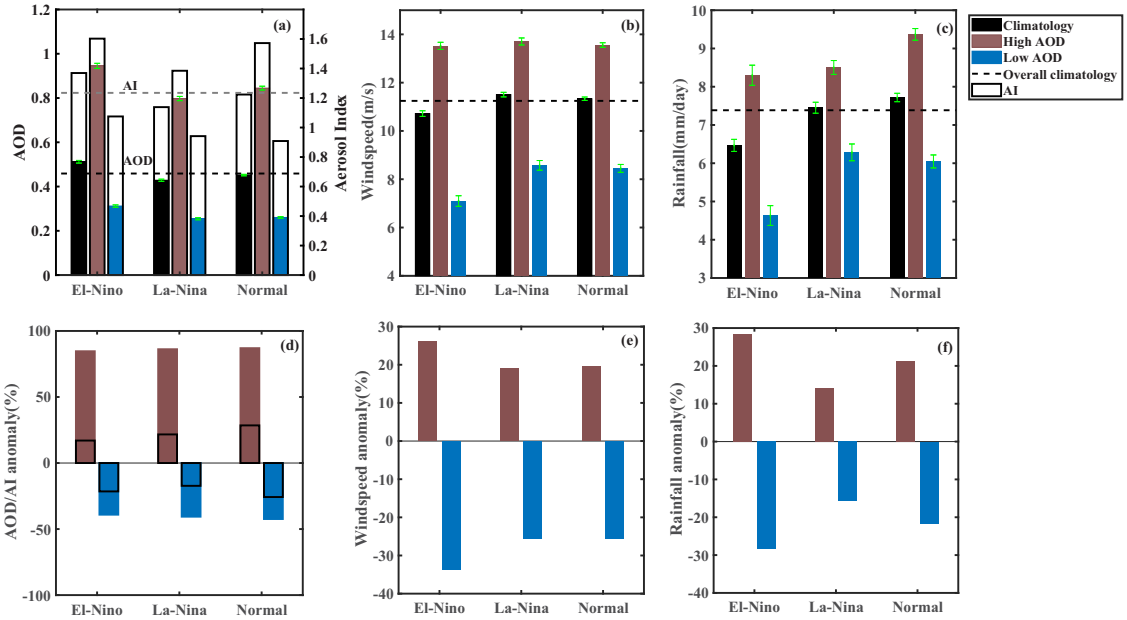

Fig. 3 Response of AOD/AI, winds over AS and rainfall over CI to high and low aerosol loading conditions over the AS. a Mean of AOD (filled) and AI (unfilled), **b** wind speed over AS, **c** rainfall over CI for the three phases of ENSO considering the climatology and the high/low aerosol loading conditions. **d** AOD/AI, **e** wind speed, **f** rainfall, anomalies in terms of percentage w.r.to the climatology of corresponding ENSO phase. The black dashed lines correspond to overall climatology considering all years.

link between AS/West Asian dust and monsoon rainfall is robust and exists during all phases of ENSO. It is also interesting to observe the enhancement and reduction of correlation during El-Nino and La-Nina respectively. These phases of ENSO are typically associated with drought/lower rainfall (during El-Nino) and flood/higher rainfall (during La-Nina) over the Indian region. Thus, there is a contrast in the correlation patterns and the overall rainfall changes over India, associated with ENSO. When one weakens the prevalent seasonal rain, the other strengthens the coupling between aerosols over the AS and rainfall over CI on short time scales. Figure 2d indicates that the relative value of correlation and mean AI during different ENSO phases are similar. Both peak during El-Nino and decrease during La-Nina. The variability in AI (as seen in error bars) also follows a similar pattern indicating the tight coupling between large-scale oscillations such as ENSO, dust emission over the Arabian region, transport to the AS, and rainfall over the CI region.

Further analysis was carried out by separating these periods based on high and low aerosol loading conditions over the AS during different ENSO phases. It may be cautioned that the strong relationship between ENSO-related circulation and the West Asian/AS aerosol-monsoon correlation does not in any way negate the dust-induced short period rainfall enhancement discussed by the previous investigators[21,22,24,45].

Changes in AOD, wind speed and rainfall

Further analysis is carried out to elucidate how rainfall over CI and wind speed over the AS changes corresponding to different aerosol loading conditions (low and high) within different phases of ENSO (Fig. 3). The high AOD period is those days with AOD greater than the 80th percentile of the daily time series. Similarly, the low AOD period is those days with AOD lesser than the 20th percentile of the daily time series. The segregation of both high and low AOD days is done separately for each ENSO phase; please refer to the data and method section for more details.

Figure 3a shows the mean AOD during high and low aerosol loading conditions and the mean AOD climatology (i.e. considering both high and low aerosol loading periods) for each ENSO phase. Interestingly, in both climatology and high loading conditions, the values of AOD and AI follow the pattern observed for the correlation discussed earlier, i.e. the highest values correspond to El-Nino, followed by Normal and La-Nina years. However, neither climatological wind speeds over the AS nor the climatological rainfall over the CI follows the correlation's relative magnitude (Fig. 3b, c). This indicates that the correlation follows the overall aerosol loading over the AS, implying that high dust/aerosol presence is crucial for the observed correlation and changes.

The highest climatological winds are observed during La-Nina, followed by Normal and El-Nino years. On the other hand, the highest rainfall is observed during the Normal period, followed by La-Nina and El-Nino years. It may be noted that past studies considering the entire Indian region showed surplus rainfall during La-Nina and droughts during El-Nino. However, this work focuses only on the CI rainfall. Hence, these slight discrepancies may result from regional differences in the rain and their modulation by large-scale ENSO phases. However, the crucial observation in the above analysis is that the AS aerosol-monsoon correlation is mainly linked to the climatological mean of aerosol loading. This is in concurrence with previous studies that showed that sufficient dust loading is an essential prerequisite for this correlation to be strong[21].

So far, the discussions are primarily based on the climatological mean of AOD, wind speed and rainfall. The overall meteorology and corresponding circulation are expected to differ during different ENSO phases. This may also partly explain why mean wind speed and rainfall do not follow the same pattern as correlation during different phases of ENSO. Therefore, comparing the wind speed and rain directly may not be ideal. To bring all these changes in mean AOD, wind speed, and rainfall corresponding to different ENSO phases into a common framework, the same analysis was also carried out using anomalies represented by changes w.r.to their respective climatologies (see Fig. 3d-f). It is observed that AOD anomalies for high and low loading conditions are as high as 80% and as low as 40%. Whereas the same for AI is ~±30%. However, the highest value of AOD anomaly corresponds to Normal years followed by La-Nina and El-Nino.

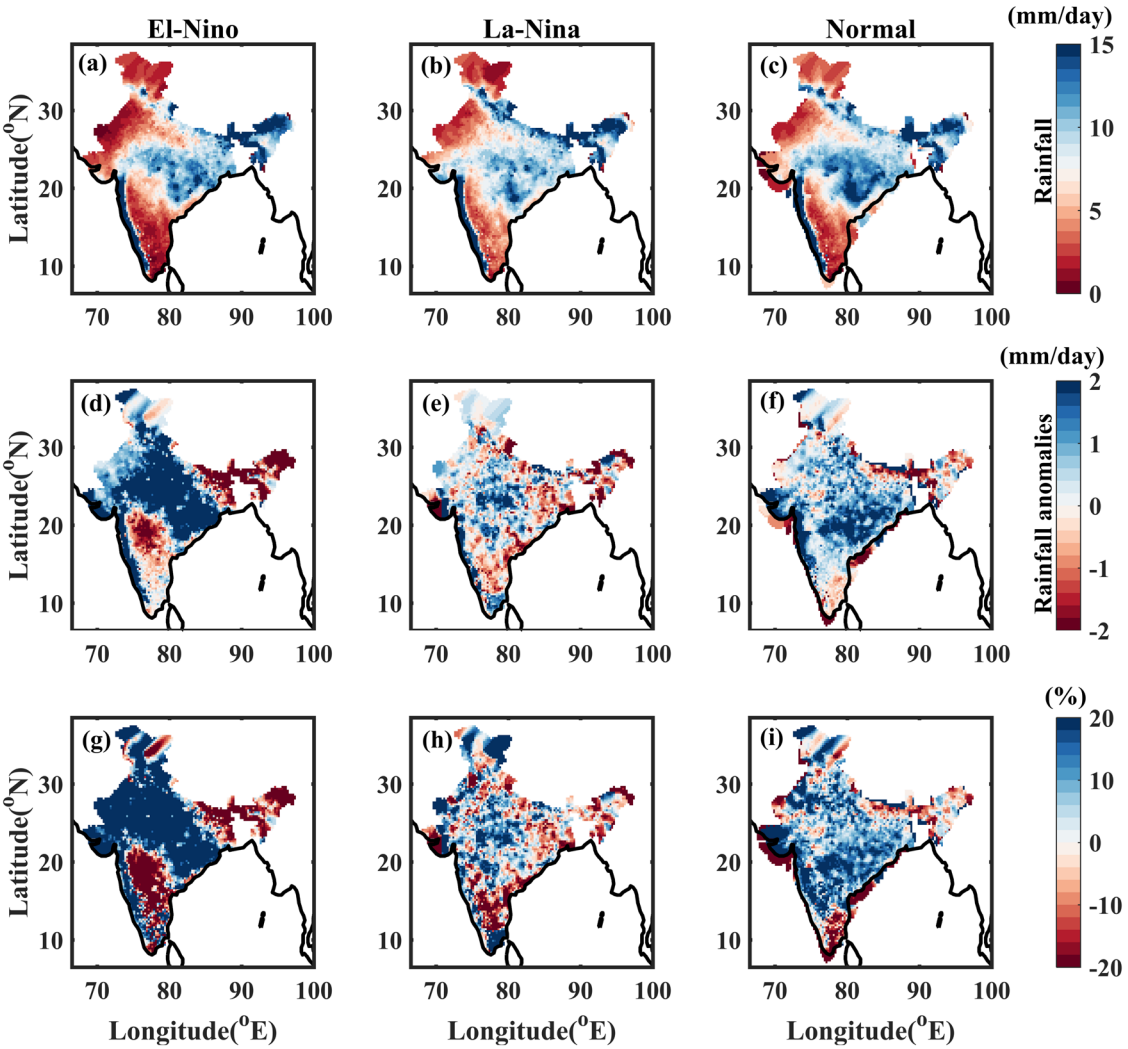

Fig. 4 Rainfall over India during El-Nino, La-Nina and Normal years. a–c climatological rainfall (mm day-1) pattern, **d–f** rainfall anomalies, **g–i** rainfall anomalies expressed in terms of percentages.

A similar analysis for wind speed and rainfall anomalies reveals an interesting pattern. The anomalies of wind speed and rainfall are negative during low AOD and positive during high AOD for different phases of ENSO. They (for both high and low loading conditions) follow the correlation (shown in Fig. 2d) with the highest anomalies corresponding to El-Nino followed by Normal and La-Nina years. Rather than the exact numbers, the relative magnitude of wind speed and rainfall between the different ENSO phases is relevant here. Thus, these apparent relationships between correlation, dust/aerosol loading, the anomaly of wind speed and rainfall indicate strong coupling between each other. The direction of these coupling (what leads to what) has been the subject of many past studies[46,47]. Hence, further discussions will explain the concurrent changes in regional rainfall, circulation and moisture convergence.

The increase/decrease in wind speed/rainfall obtained for different phases of ENSO and aerosol loading conditions within each phase may not be attributed to dust aerosols over the AS alone. A positive anomaly of 30% in rainfall should not be construed as a response driven by aerosols alone but as an overall response due to changes in large-scale circulation and the potential feedback from dust aerosols. Previously, model simulations[45] revealed that an enhancement of dust emission over the West Asian region increases the rainfall over India by 0.20–0.40 mm/day. Thus, an enhancement in dust aerosol loading indicated by higher AI/AOD over the AS may positively affect the ISMR. Earlier studies have shown overall dust-induced feedback in rainfall of ~6[21]–10%[24,45]. Thus, any environmental condition favoring high dust aerosol over the AS will lead to short period enhancement in rainfall and thus enhance this correlation. It is known that the rainfall over CI lags behind aerosol loading conditions over the AS by 7–12 days[21,24], and hence this information has also been incorporated in the analysis by extracting (and averaging) rainfall with a lag of 7–12 days w.r.to aerosol loading.

The later sections will explore the spatial pattern of the changes in winds, moisture convergence and rain corresponding to high aerosol loading conditions within each ENSO phase.

The rainfall pattern and its changes during high AOD

Past studies have confirmed the impact of remote dust radiative forcing in modulating the monsoon rainfall[21–23]. However, all these results slightly differ in terms of the resulting spatial pattern of the rainfall. One study observed increased rainfall over the whole Indian region except South-East[22]. Another study using a Regional Climate Model (RCM) suggested that the dust aerosols could increase South India's rainfall but decrease rainfall over Central and North India[23]. As pointed out earlier, the potential effect of dust aerosols on rainfall strengthens with the loading of

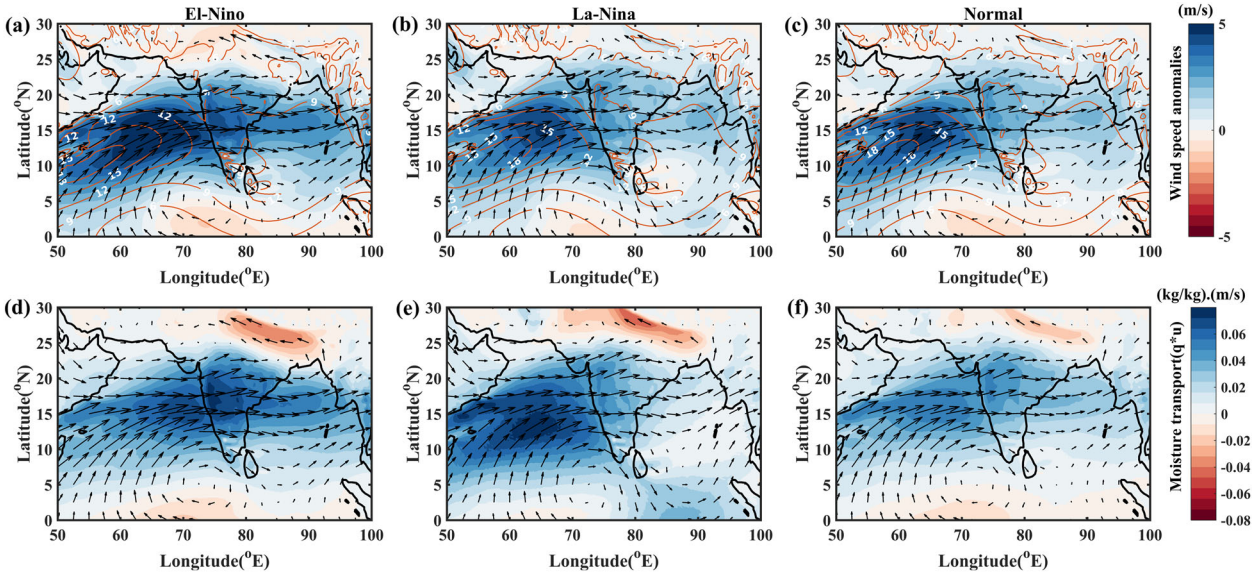

Fig. 5 Changes in wind pattern and moisture transport over the AS. a–c The contour shows the climatological wind speed, the colour bar shows the wind speed anomalies during high AOD over the AS w.r.to climatology, the vector shows the anomalies in wind direction. **d–f** The colour bar indicates moisture transport anomalies at 850 hPa level (q*u), the vector shows wind direction anomalies.

aerosols over the AS. Therefore, only the spatial pattern of rain corresponding to high dust conditions is shown here.

We analyzed the spatial distribution of climatological rainfall (Fig. 4a-c) and anomalies (Fig. 4d-i) during high loading conditions. The rainfall over India during high aerosol loading conditions over the AS is widespread across India, with the highest increase over the North, Central and North-Western India except the rain shadow region to the East of the Western Ghats. In climatology, the spatial pattern of rainfall is similar during all three phases, with the anomalies comparatively higher during El-Nino followed by Normal and La-Nina. It is also found that spatial heterogeneity of rainfall anomalies is highest during La-Nina during high aerosol loading conditions indicating that the increase/decrease in rainfall is not as homogeneous compared to El-Nino and Normal years. The obtained results are consistent with past findings[21,22]. Thus, the increased aerosol loading over the AS is also associated with increased rainfall over large swaths of land area over the Indian region where the monsoon is active and not just over CI. This indicates there is no specific regional selectivity in enhancing rainfall over India associated with high dust/aerosols over the AS, especially during El-Nino and La-Nina. However, one crucial difference is the enhancement in the rain covering the Northern part of Peninsular India during the Normal years w.r.to El-Nino and La-Nina years. In addition, there also appears to be an asymmetry between rainfall responses over most of India and North-East (NE) India. It is currently unclear why this difference exists. Overall, the El-Nino period with high aerosol loading over the AS is associated with a significant enhancement in rainfall over wet regions excluding NE India. The Normal years with high aerosol loading over the AS are associated with more widespread rain over India, especially in the Southern Peninsular region.

Concurrent changes in winds and moisture transport

The climatological wind pattern during monsoon has its maximum wind speed over the region around 5–15°N and 50–60°E in the AS. The area of maximum wind speed is shifting northeastward (10–15°N and 60–70°E) towards the Indian mainland during high aerosol loading conditions. The spatio-temporal average of mean wind speed (shown in Fig. 3b) for high aerosol loading conditions is similar for all the different phases of ENSO. However, the spatial distribution (Fig. 5) of climatological wind speed reveals marked differences in patterns with large spatial extent during La-Nina and least during El-Nino. While considering high AOD conditions, the highest enhancement in winds (with large spatial extent) is observed during El-Nino, followed by Normal and La-Nina. This is subsequently also related to enhanced moisture transport (Fig. 5d-f) during high dust episodes, potentially resulting in increased rainfall. High moisture transport regions also spread across the CI region during El-Nino years compared to La-Nina (where the enhancement is significant over the AS but does not get extended over the CI region) and Normal years (Fig. 5d–f).

A study was conducted to analyze the causality of the positive correlation obtained by Vinoj et al. [21] between dust aerosols over the AS and rainfall over CI[46]. They concluded that the increased precipitation over CI is associated with a cyclonic circulation over the Bay of Bengal. The northwesterly winds transporting the dust aerosols to the AS are part of this regional circulation and are thus interlinked. Their study suggests that maximum AOD over the AS is seen days before the maximum precipitation over CI and concludes that dust direct radiative forcing may not necessarily lead to these correlations. From this study, it is clear that though wind speeds are almost similar for high aerosol loading conditions for all the ENSO phases, the rainfall anomalies exhibit a distinct pattern (with the highest increase in rainfall for El-Nino followed by Normal and La-Nina years) and this pattern (see Fig. 3f) matches the aerosol loading (dust indicated by AI) pattern over the AS corresponding to different ENSO phases (see Fig. 2d). If winds, dust, and rainfall are all interlinked to a single exogenous factor, the anomalies of all these parameters should also have followed each other. However, Fig. 3 shows that this is not the case. Also, the anomalies of both winds and rainfall follow the climatological aerosol loading rather than its anomalies. This may indicate more complex interactions between these parameters over this region that are not evident directly from observations. Thus, it appears that the overall dust loading is a much more vital component than the anomalies induced by changes in winds, as indicated by certain studies[46]. It may be stated that though circulation may be affecting the dust loading[46], the dust has its own feedback effect[21], through which it influences rainfall over India. Thus it may be stressed that external factors such as large-scale oscillations as discussed in this paper and those pointed out by other studies[46,47] do not negate the possibility of dust-induced

feedback. Instead, these circulation changes induced by regional features (such as monsoon depressions) or ENSO may enhance the overall dust loading over the AS, thereby causing changes to CI rainfall. Interestingly, even under conditions where droughts are expected (El-Nino period), the rainfall increases over CI during high aerosol loading conditions indicating that the AS dust effect is important, significant and discernible.

METHODS

Data

We have used the long-term AOD during the period 1981–2013 from National Oceanic and Atmospheric Administration – Advanced Very High-Resolution Radiometer (NOAA-AVHRR) ($0.1° \times 0.1°$)[48], Moderate Resolution Imaging Spectroradiometer (MODIS) onboard the Terra (Aqua) satellites ($1.0° \times 1.0°$) during the period 2000–2013 (2002–2013)[49], Modern-Era Retrospective analysis for Research and Application (MERRA-2) ($0.625 \times 0.5°$)[46] during the period 1981–2013 over South Asian domain along with daily gridded rainfall data from the Indian Meteorological Department ($0.25 \times 0.25°$) over the CI region (16.5–26.5°N and 74.5–86.6°E)[50] to explore the AS dust and ISMR correlation. In addition, Aerosol Index (AI) measured using the instrument TOMS (Total Ozone Mapping Spectrometer) onboard the satellites Nimbus-7 (1981–1993), Earth Probe (1996–2004), and the instrument OMI (Ozone Mapping Spectrometer) onboard Aura (2005–2013) is also used[51]. To understand the circulation features and moisture transport, the zonal and meridional winds, and specific humidity at 850 hPa level are obtained from the ERA5 reanalysis data with a resolution of $0.25° \times 0.25°$ during the period 1981–2013[52]. All data are obtained at daily temporal resolution. The AVHRR is one of the earliest sensors used to retrieve aerosol optical depth from measurements in the visible and near-infrared, beginning in the late 1970s. AVHRR orbits the Earth at an altitude of 833.0 km and has a swath width of 2399.0 km. The instrument observes Earth in six wavelengths from 0.58 to 12.5 μm[48]. The aerosol products from MODIS onboard the Aqua and Terra satellites are extensively studied and validated[49–51]. However, this data are available only since 2000 (Terra) and 2002 (Aqua), respectively. MERRA-2 is a chemical reanalysis product that is widely used and is created through satellite data assimilation and validation by the National Atmospheric and Space Administration (NASA). Due to its unique retrieval methodology, TOMS AI is highly sensitive to absorbing aerosols (e.g. dust and black carbon). It is also one of the longest and most widely used satellite measurement products available for scientific research activities.

Correlation analysis

The correlation between the AS aerosols and CI monsoon rainfall is calculated using the following two methodologies. The AOD retrievals from satellites during monsoon are sparse due to frequent cloudiness. Therefore, we have followed a strategy to use weekly mean AOD maps (at each grid) and weekly mean (spatially averaged) central Indian rainfall as a time series. During the monsoon period (June–September), these time series are used as two independent variables that are then correlated with each other using the widely used Pearson's correlation coefficient (see the result in Fig. 1). The above analysis follows the methodology developed by an earlier study[21]. The second method concerns calculating the Pearson's correlation coefficient between AS AOD and CI rainfall for the different phases of ENSO (see the next section for their definition). In this case, the AVHRR-AOD values over the region having maximum correlation in the AS (10–25°N and 50–75°E) based on Fig. 1 are spatially averaged to obtain the weekly mean time series of AOD. These weekly time series of AOD are then used to estimate the correlation coefficient with CI rainfall (shown in Fig. 2d) during different phases of ENSO. The statistical significance is calculated using the standard student's t-test.

Identification of ENSO phases

The El-Nino, La-Nina and Normal years are classified based on the Oceanic Nino Index (ONI) calculated by the NOAA's Climate Prediction Center[53]. Oceanic Nino index is a 3-month running mean of SST anomalies over the Nino 3.4 region (5°N–5°S and 120°–170°W) calculated based on the Extended Reconstructed SST Version 4 (ERSSTv4) dataset[54]. The SST anomalies are defined as the departure of SST values from the average of the centred 30-year base period updated every five years. The years with the 3-month running mean of SST anomalies during June to August (JJA) and July to September (JAS) greater than or equal to 0.5 °C (lesser than or equal to −0.5 °C) are classified as El-Nino (La-Nina), and the remaining years as Normal.

Identification of high/low Aerosol loading conditions

To develop composite features of winds, rainfall, and moisture transport, the daily AVHRR-AOD values over the region having maximum correlation in the AS (10–25°N and 50–75°E) based on Fig. 1 are spatially averaged to obtain the time series of AOD. The time series (4 months each for 33 years) is separated into El-Nino, La-Nina and Normal years. Then, the data corresponding to different ENSO phases is further segregated based on a percentile-based analysis (80th percentile and above for high loading and 20th percentile and below for low loading conditions) into high and low loading days. The corresponding dates of these high/low aerosol loading periods are used to perform the composite analysis concerning Figs. 3, 4 and 5.

DATA AVAILABILITY

All data used in the current work are in the public domain. The specific links are provided in the acknowledgement section.

CODE AVAILABILITY

The analysis was carried out, and the figures were generated using matlab2015b (https://in.mathworks.com/). The same may be shared on reasonable request.

Received: 11 March 2021; Accepted: 21 February 2022;
Published online: 28 March 2022

REFERENCES

1. Atwater, M. A. Planetary albedo changes due to aerosols. *Science* **170**, 64–66 (1970).
2. Ramanathan, V. et al. Indian Ocean experiment: an integrated analysis of the climate forcing and effects of the great Indo-Asian haze. *J. Geophys. Res.* **106**, 28371–28398 (2001).
3. Satheesh, S. & Ramanathan, V. Large differences in tropical aerosol forcing at the top of the atmosphere and Earth's surface. *Nature* **405**, 60–63 (2000).
4. Hansen, J., Sato, M. & Ruedy, R. Radiative forcing and climate response. *J. Geophys. Res. Atmos.* **102**, 6831–6864 (1997).
5. Twomey, S. The influence of pollution on the shortwave albedo of clouds. *J. Atmos. Sci.* **34**, 1149–1152 (1977).
6. Albrecht, B. A. Aerosols, cloud microphysics, and fractional cloudiness. *Science* **245**, 1227–1230 (1989).
7. Meehl, G. A., Arblaster, J. M. & Collins, W. D. Effects of black carbon aerosols on the Indian monsoon. *J. Clim.* **21**, 2869–2882 (2008).
8. Srivastava, A. K. et al. Pre-monsoon aerosol characteristics over the Indo-Gangetic Basin: implications to climatic impact. *Ann. Geophys.* **29**, 789–804 (2011).
9. Ganguly, D., Rasch, P. J., Wang, H. & Yoon, J. H. Fast and slow responses of the South Asian monsoon system to anthropogenic aerosols. *Geophys. Res. Lett.* **39**, 1–5 (2012).
10. Pandey, S. K., Vinoj, V., Landu, K. & Babu, S. S. Declining pre-monsoon dust loading over South Asia: signature of a changing regional climate. *Sci. Rep.* **7**, 16062 (2017).
11. Sarangi, C., Kanawade, V. P., Tripathi, S. N., Thomas, A. & Ganguly, D. Aerosol-induced intensification of cooling effect of clouds during Indian summer monsoon. *Nat. Commun.* **9**, 3754 (2018).
12. Maharana, P., Dimri, A. P. & Choudhary, A. Redistribution of Indian summer monsoon by dust aerosol forcing. *Meteorol. Appl.* **26**, 584–596 (2019).
13. Wang, C., Kim, D., Ekman, A. M. L., Barth, M. C. & Rasch, P. J. Impact of anthropogenic aerosols on Indian summer monsoon. *Geophys. Res. Lett.* **36**, L21704 (2009).
14. Ramanathan, V. et al. Atmospheric brown clouds: impacts on South Asian climate and hydrological cycle. *Proc. Natl Acad. Sci. USA* **102**, 5326–5333 (2005).
15. Lau, K. M. & Kim, K. M. Observational relationships between aerosol and Asian monsoon rainfall, and circulation. *Geophys. Res. Lett.* **33**, 1–5 (2006).
16. Lau, K. M., Kim, M. K. & Kim, K. M. Asian summer monsoon anomalies induced by aerosol direct forcing: the role of the Tibetan Plateau. *Clim. Dyn.* **26**, 855–864 (2006).
17. Kuhlmann, J. & Quaas, J. How can aerosols affect the Asian summer monsoon? Assessment during three consecutive pre-monsoon seasons from CALIPSO satellite data. *Atmos. Chem. Phys.* **10**, 4673–4688 (2010).

18. Wonsick, M. M., Pinker, R. T. & Ma, Y. Investigation of the 'elevated heat pump' hypothesis of the Asian monsoon using satellite observations. *Atmos. Chem. Phys.* **14**, 8749–8761 (2014).
19. Nigam, S. & Bollasina, M. 'Elevated heat pump' hypothesis for the aerosol-monsoon hydroclimate link: 'Grounded' in observations? *J. Geophys. Res. Atmos.* **115**, 4–10 (2010).
20. Lau, K. M. & Kim, K. M. Comment on "'Elevated heat pump' hypothesis for the aerosol - monsoon hydroclimate link: 'Grounded' in observations?" by S. Nigam and M. Bollasina. J. Geophys. Res. Atmos. **116**, 4–7 (2011).
21. Vinoj, V. et al. Short-term modulation of Indian summer monsoon rainfall by West Asian dust. *Nat. Geosci.* **7**, 308–313 (2014).
22. Jin, Q., Jiangfeng, W. & Zong-Liang, Y. Positive response of Indian summer rainfall to Middle East dust. *Geophys. Res. Lett.* **64**, 1180–1188 (2014).
23. Solmon, F., Nair, V. S. & Mallet, M. Increasing Arabian dust activity and the Indian summer monsoon. *Atmos. Chem. Phys.* **15**, 8051–8064 (2015).
24. Jin, Q., Wei, J., Yang, Z.L., Pu, B. & Huang, J. Consistent response of Indian summer monsoon to Middle East dust in observations and simulations. *Atmos. Chem. Phys.* **15**, 9897–9915 (2015).
25. Singh, C., Ganguly, D. & Dash, S. K. Dust load and rainfall characteristics and their relationship over the South Asian monsoon region under various warming scenarios. *J. Geophys. Res.* **122**, 7896–7921 (2017).
26. Sikka, D. R. Some aspects of the large-scale fluctuations of summer monsoon rainfall over India in relation to fluctuations in planetary and regional scale circulation parameters. *Proc. Indian Acad. Sci. Earth Planet Sci.* **89**, 179–195 (1980).
27. Webster, P. J. & Yang, S. Monsoon and Enso: selectively interactive systems. *Q. J. R. Meteorol. Soc.* **118**, 877–926 (1992).
28. Banerjee, P. & Kumar, S. P. ENSO modulation of interannual variability of dust aerosols over the northwest Indian Ocean. *J. Clim.* **29**, 1391–1415 (2016).
29. Abish, B. & Mohanakumar, K. Absorbing aerosol variability over the Indian subcontinent and its increasing dependence on ENSO. *Glob. Planet. Change* **106**, 13–19 (2013).
30. Kim, M. K. et al. Amplification of ENSO effects on Indian summer monsoon by absorbing aerosols. *Clim. Dyn.* **46**, 2657–2671 (2016).
31. Fadnavis, S., Roy, C., Sabin, T. P., Ayantika, D. C. & Ashok, K. Potential modulations of pre-monsoon aerosols during El Niño: impact on Indian summer monsoon. *Clim. Dyn.* **49**, 2279–2290 (2017).
32. Freund, M. B. et al. Higher frequency of Central Pacific El Niño events in recent decades relative to past centuries. *Nat. Geosci.* **12**, 450–455 (2019).
33. Wang, B. et al. Historical change of El Niño properties sheds light on future changes of extreme El Niño. *Proc. Natl Acad. Sci. USA* **116**, 22512–22517 (2019).
34. Jin, Q., Wei, J., Pu, B., Yang, Z. L. & Parajuli, S. P. High summertime Aerosol loadings over the Arabian Sea and their transport pathways. *J. Geophys. Res. Atmos.* **123**, 10,568–10,590 (2018).
35. Satheesh, S. K., Vinoj, V. & Krishnamoorthy, K. Assessment of Aerosol radiative impact over Oceanic regions adjacent to Indian subcontinent using multisatellite. *Anal. Adv. Meteorol.* **2010**, 1–13 (2010).
36. Vinoj, V. & Satheesh, S. K. Measurements of aerosol optical depth over Arabian Sea during summer monsoon season. *Geophys. Res. Lett.* **30**, 67–70 (2003).
37. Mooley, D. A. & Parthasarathy, B. Indian summer monsoon and El Nino. *Pure Appl. Geophys. pageoph* **121**, 339–352 (1983).
38. Rajeevan, M. & Pai, D. S. On the El Niño-Indian monsoon predictive relationships. *Geophys. Res. Lett.* **34**, 1–4 (2007).
39. Surendran, S., Gadgil, S., Rajendran, K., Varghese, S. J. & Kitoh, A. Monsoon rainfall over India in June and link with northwest tropical pacific. *Theor. Appl. Climatol.* **135**, 1195–1213 (2019).
40. Chakraborty, A. Preceding winter la Niña reduces Indian summer monsoon rainfall. *Environ. Res. Lett.* **13**,054030 (2018).
41. Gadgil, S. & Francis, P. A. El Niño and the Indian rainfall in June. *Curr. Sci.* **110**, 1010–1022 (2016).
42. Hoell, A., Funk, C. & Barlow, M. The regional forcing of Northern hemisphere drought during recent warm tropical west Pacific Ocean La Niña events. *Clim. Dyn.* **42**, 3289–3311 (2014).
43. Wu, R., Chen, J. & Chen, W. Different types of ENSO influences on the Indian Summer Monsoon variability. *J. Clim.* **25**, 903–920 (2012).
44. Swapna, P. et al. The IITM Earth System Model: transformation of a seasonal prediction model to a long-term climate model. *Bull. Am. Meteorol. Soc.* **96**, 1351–1367 (2015).
45. Singh, C., Ganguly, D., Sharma, P. & Mishra, S. Climate response of the south Asian monsoon system to West Asia, Tibetan Plateau and local dust emissions. *Clim. Dyn.* **53**, 6245–6264 (2019).
46. Sharma, D. & Miller, R. L. Revisiting the observed correlation between weekly averaged Indian monsoon precipitation and Arabian Sea aerosol optical depth. *Geophys. Res. Lett.* **44**, 10,006–10,016 (2017).
47. Kumar, S. & Arora, A. On the connection between remote dust aerosol and Indian summer monsoon. *Theor. Appl. Climatol.* **137**, 929–940 (2019).
48. Zhao, T. X. P. et al. A study of the effect of non-spherical dust particles on the AVHRR aerosol optical thickness retrievals. *Geophys. Res. Lett.* **30**, 1–4 (2003).
49. Remer, L. A. et al. The MODIS Aerosol algorithm, products, and validation. *J. Atmos. Sci.* **62**, 947–973 (2005).
50. Pai, D. S. et al. (1901-2010) daily gridded rainfall data set over India and its comparison with existing data sets over the region. *Mausam* **1**, 1–18 (2014).
51. McPeters, R. et al. Total ozone mapping spectrometer (TOMS) Level-3 data products user's guide. *NASA Tech. Memo*. 209896 (2000).
52. Hersbach, H. et al. The ERA5 global reanalysis. *Q. J. R. Meteorol. Soc.* **146**, 1999–2049 (2020).
53. NOAA (National Oceanic and Atmospheric Administration). Climate Prediction Center(CPC), Cold and warm episodes by season. http://www.cpc.ncep.noaa.gov/products/analysis_monitoring/ensostuff/ensoyears2011.shtml. Accessed during March 2019.
54. Huang, B. et al. Extended reconstructed sea surface temperature version 4 (ERSST. v4). Part I: Upgrades and intercomparisons. *J. Clim.* **28**, 911–930 (2015).

ACKNOWLEDGEMENTS

Data used in this study were obtained from the Giovanni online data system, developed and maintained by the NASA GES DISC (https://disc.gsfc.nasa.gov/). We acknowledge the MODIS mission scientists and Principal Investigators who provided the data used in this research effort. NOAA/NCEI is acknowledged for providing the AVHRR aerosol datasets (https://www.ncdc.noaa.gov/cdr/atmospheric/avhrr-aerosol-optical-thickness). In addition, ECMWF (https://cds.climate.copernicus.eu/cdsapp#!/dataset/reanalysis-era5-single-levels)/ and MERRA-2 (https://gmao.gsfc.nasa.gov/reanalysis/MERRA-2/) reanalysis acknowledged for the products they provided. V.V. thanks the Indian Space Research Organization's Aerosol Radiative Forcing over India (ISRO-ARFI) for funding some aspects of this work through its ARFINET program. G.N. acknowledge the Prime Minister Research Fellowship (PMRF) program for supporting her doctoral research. We acknowledge partial support from the DST-SPLICE climate change program through project code DST/CCP/NUC/148/2018.

AUTHOR CONTRIBUTIONS

V.V. and G.N. conceived the ideas. G.N. carried out all analyses and wrote the first draft of the manuscript with equal contribution from all co-authors.

COMPETING INTERESTS

The authors declare no competing interests.

ADDITIONAL INFORMATION

Correspondence and requests for materials should be addressed to V. Vinoj.

Reprints and permission information is available at http://www.nature.com/reprints

Publisher's note Springer Nature remains neutral with regard to jurisdictional claims in published maps and institutional affiliations.